

Synthesis and Photoluminescence Behavior of the Eu^{3+} Ions as a Nanocoating over a Silica Stöber Matrix

Ieda L. V. Rosa · Larissa H. Oliveira · Elson Longo · José A. Varela

Received: 27 October 2009 / Accepted: 29 April 2010 / Published online: 9 May 2010
© Springer Science+Business Media, LLC 2010

Abstract In this work, a SiO_2 spherical were prepared by the Stöber Method and then recovered with a single layer of Eu_2O_3 oxide ($\text{SiO}_2@\text{Eu}_2\text{O}_3$) obtained by the Polymeric Precursor Method. The $\text{SiO}_2@\text{Eu}_2\text{O}_3$ powder was heated treated at 100, 300, 400, 500 and 800 °C. The samples were characterized by the Scanning Electronic Microscopy (SEM), Thermal Analysis (TGA/DTA), and the luminescent properties of the $\text{SiO}_2@\text{Eu}_2\text{O}_3$ powders were studied by their emission and excitation spectra as well as by the lifetime measurements of the $\text{Eu}^{3+} {}^5\text{D}_0 \rightarrow {}^7\text{F}_2$ transition. The SEM analysis shows that the silica prepared by the Stöber Method is spherical with a particle size of 460 nm. The emission spectra of the $\text{SiO}_2@\text{Eu}_2\text{O}_3$ powders presented the Eu^{3+} characteristics bands related to the ${}^5\text{D}_0 \rightarrow {}^7\text{F}_J$ ($J=0, 1, 2, 3, 4$) transitions at 577, 591, 616, 649 and 695 nm, respectively. The band related to the ${}^5\text{D}_0 \rightarrow {}^7\text{F}_2$ transition is the most intense in the spectra, and its intensity decreases with the temperature enhancement. The decay curves of the $\text{SiO}_2@\text{Eu}_2\text{O}_3$ samples presented monoexponential features, and the obtained lifetime values were higher than the Eu_2O_3 oxide. It was possible to conclude that the ${}^5\text{D}_0 \rightarrow {}^7\text{F}_2$ hypersensitive transition is strongly dependent on the Eu^{3+} surrounding.

Keywords Europium · Luminescence · SiO_2 · Nanocoating · Photoluminescence properties

I. L. V. Rosa (✉) · L. H. Oliveira
Department of Chemistry, LIEC-UFSCar,
Caixa Postal 676, 13560-905 São Carlos, SP, Brazil
e-mail: ilvrova@ufscar.br

E. Longo · J. A. Varela
LIEC-UNESP, Institute of Chemistry,
Caixa Postal 355, 14801-970 Araraquara, SP, Brazil

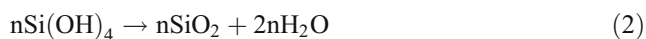
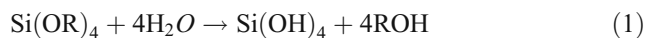
Introduction

Since the fifties, materials have been synthesized by different methodologies. In this search for new luminescent materials, the Eu^{3+} ion was incorporated in several matrixes [1] such as Y_2O_3 , YVO_4 , $\text{La}(\text{BO}_3)_3$, or YNbO_4 , and the studies for controlling and arise their luminescent properties has just started through the comprehension of the interaction between the rare earth ions and the matrix [2].

The silica is one of the most inorganic substances used as support for several systems with application in many areas. The main silica property is related to its surface that can be used in the immobilization of rare earth compounds. These rare earth ions can recover the silica particles aiming the obtention of a “core-shell” luminescent material where the particle size is controlled by the silica, with the specific objective of increasing the packaging, decreasing the scattering of light, to increase the intensity of luminescence and improve its definition [3–5].

The synthesis of spherical and monodisperse silica particles was described by STÖBER *et al* [6]. These silica particles were prepared by the hydrolysis of tetraethylorthosilicate (TEOS) in a mixture of alcohol, water and ammonia. The hydrolysis can be performed using an acid condition, but a basic condition is in general more used. The hydrolysis of alkoxysilanes occurs by a nucleophilic mechanism, where under basic conditions the water dissociates to produce nucleophilic hydroxyl anions (OH^-) in a rapid first step, and then the hydroxyl anion attacks the silicon atom. When an alkoxide group (OR^-) is replaced by a hydroxyl group the others alkoxide groups are also replaced giving rise to the $\text{Si}(\text{OH})_4$. The second step of this reaction is the condensation of the $\text{Si}(\text{OH})_4$ when the spherical silica particles are formed. The hydrolysis and the condensation mechanisms of an alkoxysilane are presented

in the Equations (1) and (2) as follow [7]:



The excellent spherical silica particles monodispersivity turns out the Stöber Method widely studied in the obtention of this kind of material. It is necessary to control some reaction conditions such as temperature, pH, reagent concentration and homogenization to promote a faster nucleation and a uniform growth of the particles. The silica obtained by this method presents a reticule structure with Si-O-Si linkages into the particles and silanols groups Si-OH in its surface [8].

The “core-shell” particles comprehend a new class of composites, which consists of a “core” generally involved by a nanometric “shell”. In the same way, the core material and the shell nanometric layer can be polymers, inorganic solids, metals or bio-molecules. In the literature, they are symbolized as core@shell [4, 5].

A core shell luminescent material receives considerable attention because of their luminescent property that is important to some photoelectronic devices, such as laser materials and luminescence labels and in efficient light-conversion molecular devices (LCMDs), organic light-emitting devices (OLEDs), fluorescent lamps and cathode-ray tubes, and plasma display panels (PDPs), but also in biotechnological fields [9, 10].

Their importance in biotechnological applications are related to some improvents in sensitivity, selectivity, and multicomplexing capacity over conventional fluorophores. A lanthanide doped the silica spheres can also be an efficient and cheap visible light detectors, which can offers much better performances than the infrared ones [11].

Besides the Pechini Method, others experimental procedures were used to prepare these luminescent materials, as in situ polymerization [12], layer by layer technique [13], auto construction directed by template [14], sonochemical method [15], and so one.

YU *et al.* [4], synthesized silica particles encapsulated with $\text{YVO}_4:\text{Eu}^{3+}$ by the Pechini Method, where the luminescent properties of the obtained material were studied. Through the obtained results, it was verified an enlargement of the shell crystallinity with the annealing temperature, promoting an increase of the electromagnetic radiation intensity emitted by the material. Another important factor in the luminescent properties was the shell quantity around the silica. Another encapsulated luminescent [16] material synthesized by this process was the $\text{SiO}_2@\text{CaMoO}_4:\text{Eu}^{3+}$. JIA *et al.* [17], encapsulated silica particles with the $\text{CaWO}_4:\text{Eu}^{3+}/\text{Tb}^{3+}$ luminophors and the luminescent material $\text{SiO}_2@\text{CaWO}_4:\text{Eu}^{3+}$ presented a strong red emission at

614 nm, related to the characteristic ${}^5\text{D}_0 \rightarrow {}^7\text{F}_2$ transition of the Eu^{3+} ion, while the $\text{SiO}_2@\text{CaWO}_4:\text{Tb}^{3+}$ material presented a strong green emission at 544 nm, due to the ${}^5\text{D}_4 \rightarrow {}^7\text{F}_5$ transition of the Tb^{3+} ion.

In this work, it was used to the rare earth encapsulation the spherical silica synthesized by the Stöber Method [6]. A single Eu_2O_3 oxide shell was deposited over this silica, through a sol-gel modified method [18], giving rise to the $\text{SiO}_2@\text{Eu}_2\text{O}_3$ spherical material that was characterized by Scanning Electronic Microscopy (SEM) technique and by Thermal Analysis (TGA/DTA). The photophysical properties were studied to get information about the environment around the rare earth ion during the heat treatment. These properties were investigated through the excitation and emission spectra, and also by the lifetime measurements of the $\text{Eu}^{3+} {}^5\text{D}_0 \rightarrow {}^7\text{F}_2$ transition. The obtained results were compared with a sample prepared with the commercial FUMED silica also encapsulated with a single Eu_2O_3 shell.

Experimental procedure

Spherical silica particles synthesis

The Stöber Method [6] was employed in the spherical silica particles, synthesis, and it is based in a hydrolysis of the TEOS catalyzed by the ammonia. An amount of distilled water, ethanol and ammonia was stirred for some minutes. To this solution were added 10 mL of TEOS and the recipient was stayed under stirring for more 4 h hermetically closed. After that, the solvent was evaporated and the solid obtained was dried in an oven at 100 °C for 24 h, where it was obtained 2.0 g of spherical silica.

Synthesis of $\text{SiO}_2@\text{Eu}_2\text{O}_3$ FUMED and $\text{SiO}_2@\text{Eu}_2\text{O}_3$ spherical samples

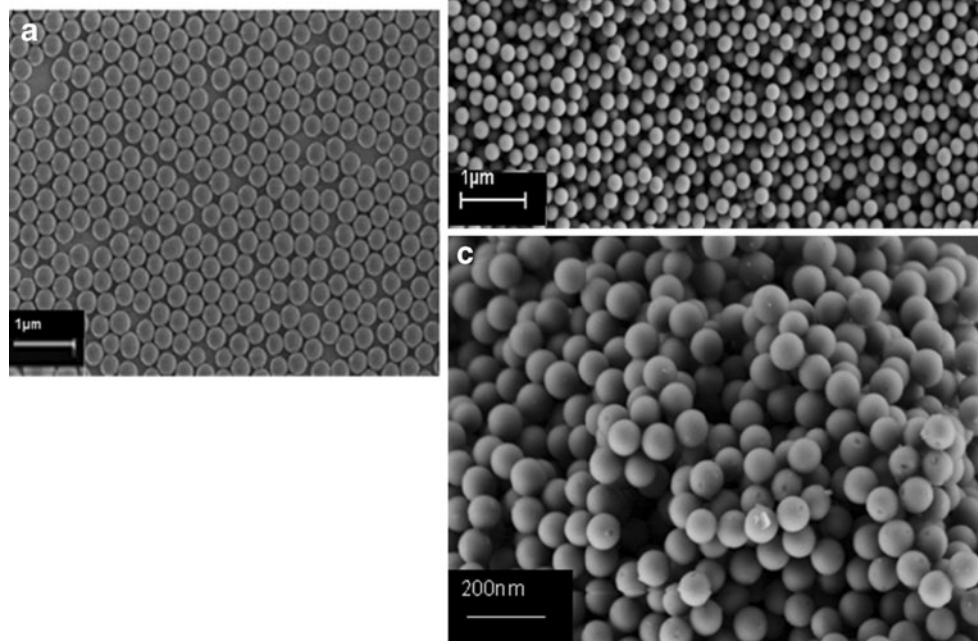
The polymeric resin used to recover the FUMED and spherical silica particles with a single shell of Eu_2O_3 was synthesized by the Polymeric Precursor Method [18]. Initially, a Eu^{3+} polymeric precursor was obtained using an aqueous Eu^{3+} citrate solution prepared from europium nitrate (europium oxide in nitric acid) and citric acid with citric acid/ metal ratio of 3/1 (mol%). Ethylene glycol was added to the citrate solution at a mass ratio of 40/60 in relation to the citric acid to produce a polymerizing reaction. The polymeric resin was used in the encapsulation after 48 h of stirring without heating. The Eu^{3+} polymeric coating an FUMED SiO_2 and spherical SiO_2 surface was prepared by a soft, chemical method, as describe elsewhere [19]. Next the suspension was dried and the obtained powder of $\text{SiO}_2@\text{Eu}_2\text{O}_3$ FUMED samples were heat

treated at 100, 300, 400, 500, and 800 °C for 2 h and the $\text{SiO}_2@\text{Eu}_2\text{O}_3$ spherical samples were treated at 100, 300, 400, 500 and 800 at a heating rate of 5 °C/min in an EDGCON 3P furnace.

Characterization

The $\text{SiO}_2@\text{Eu}_2\text{O}_3$ FUMED and $\text{SiO}_2@\text{Eu}_2\text{O}_3$ spherical materials were characterized by a field emission scanning electronic microscopy (FE-SEM), using a Supra 35-VP, Carl Zeiss, Germany microscope and by Thermal Analysis (TGA/DTA) in a Netzsch–Thermische Analyse STA 409 cell equipment using a heating rate of 5 °C/min under synthetic air atmosphere. The luminescent properties were studied through the excitation and emission spectra and also by the lifetime measurements of the $\text{Eu}^{3+} \ ^5\text{D}_0 \rightarrow \ ^7\text{F}_2$ transition. The photoluminescence (PL) data of the $\text{SiO}_2@\text{Eu}_2\text{O}_3$ FUMED and $\text{SiO}_2@\text{Eu}_2\text{O}_3$ spherical were obtained in a Jobin Yvon-Fluorolog 3 spectrofluorometer at room temperature using a 450 W xenon lamp as excitation energy source. Luminescence lifetime measurements were carried out as well using a 1934D phosphorometer coupled to the spectrofluorometer. Lifetime data of the $\ ^5\text{D}_0 \rightarrow \ ^7\text{F}_2$ state of the Eu^{3+} in samples were also obtained from its decay curve using the emission wavelength set at 612 nm and exciting wavelength set at 393 nm.

Fig. 1 Scanning Electronic Micrograph of the (a) spherical SiO_2 particles and of the $\text{SiO}_2@\text{Eu}_2\text{O}_3$ samples annealed at (b) 300 and (c) 1000 °C



Results and discussion

Scanning electron microscopy is presented as a suitable technique for the investigation of rough surfaces, because its resolution is larger than in the optical microscopy. The analysis by this technique was realized to get some information about the size and morphology of particles. Figure 1a, b and c presents the micrographies of the spherical SiO_2 sample prepared by Stöber Method [6] and the $\text{SiO}_2@\text{Eu}_2\text{O}_3$ spherical samples heat treated at 300 and 800 °C, respectively. From the micrograph of Stöber silica (Fig. 1a), it is observed that the silica particles are spherical, monodispersed and this morphology is maintained after the encapsulation (Fig. 1b and c). The samples thermally treated are also much more clustered than the non encapsulated silica. This agglomeration of particles is caused by the heat treatment procedure.

A histogram of the average size of particles was determined, since the size of these silica particles vary of some nanometers. The average size of these particles was calculated using the IMAGE J program and is presented in Fig. 2. From this graphic, almost all the silica particles presented a size of approximately 460 nm before the encapsulation. After this, it was not verified a significant change in particle size, indicating that there was only the formation of a thin film on the silica surface, which can not be identified by the microscopic techniques used in this work. From the

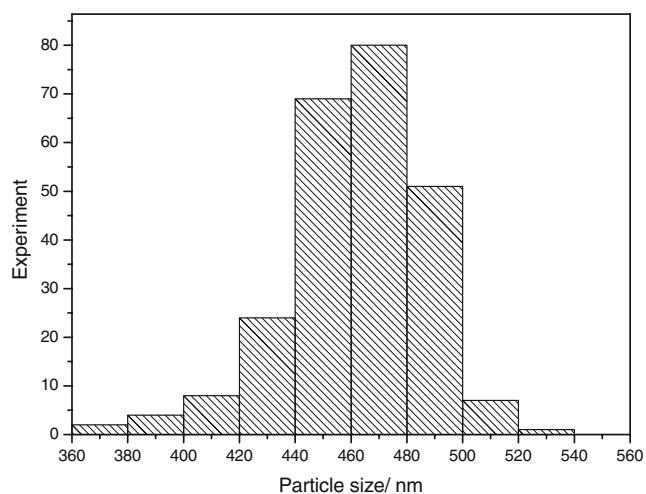


Fig. 2 Histogram representing the medium size of the Stöber silica particles

micrographies, the FUMED silica also presented a particle size much greater than the spherical silica and they are not spherical, like snowflakes, with a size of approximately 700 nm which are clustered. After the encapsulation the samples are much more clustered and its morphology remains the same as before this procedure (see Fig. 3 (a), and (b)).

The results obtained by the thermal analysis TGA/DTA (Fig. 4) of the $\text{SiO}_2@\text{Eu}_2\text{O}_3$ FUMED sample treated at 100 °C presents its thermal behavior with the temperature. In the thermogram, the curve (a) represents the mass loss during the heating of the sample from 100 to 1000 °C and curve (b) represents the results of differential thermal analysis. From these curves it is observed some transition points for this material.

The first point at 74 °C is related to an exothermic reaction which correspond a weight loss, caused by the evaporation of the water molecules on the FUMED silica surface. A second point is set from 172 to 294 °C, and corresponds to an endothermic reaction attributed to the degradation of the polymer layer containing the Eu^{3+} ion, which involves the FUMED silica. After this temperature, the material becomes thermally stable.

Fig. 3 Micrographies of the commercial FUMED silica (a) and of the $\text{SiO}_2@\text{Eu}_2\text{O}_3$ FUMED sample annealed at 500 °C (b)

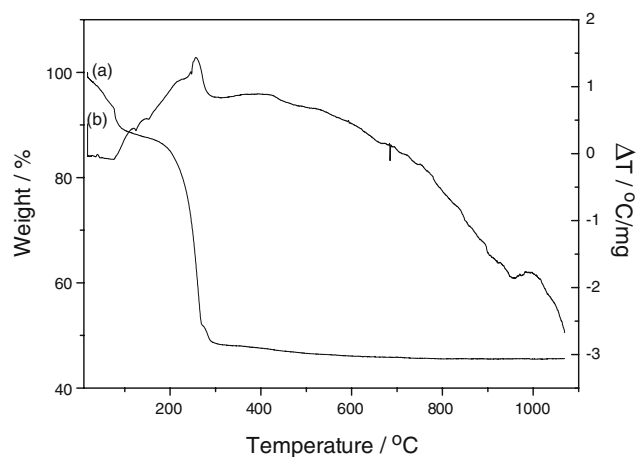
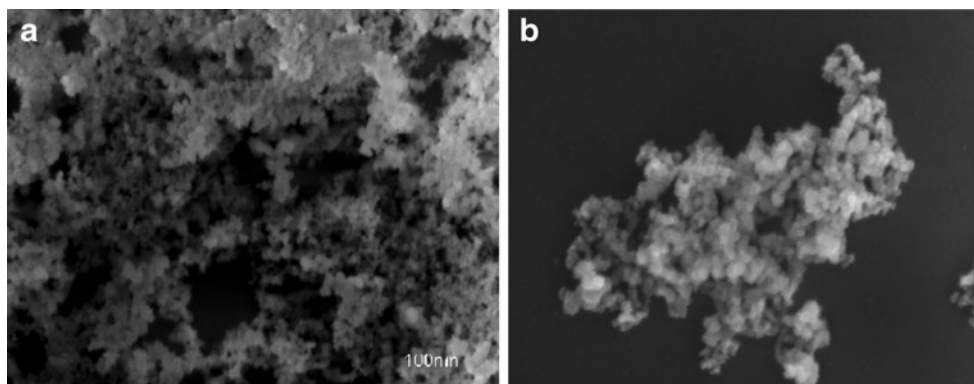


Fig. 4 (a) TGA e (b) DTA curves of the $\text{SiO}_2@\text{Eu}_2\text{O}_3$ FUMED sample annealed at 100 °C

Figure 5 presents the TGA (a) and DTA (b) curves of the $\text{SiO}_2@\text{Eu}_2\text{O}_3$ spherical sample treated at 100 °C. Through the DTA curve a transition point of an exothermic reaction at about 58 °C was noticed, which corresponds to an evaporation of water molecules on the silica surface. While the temperature increases was not observed any weight loss, indicating that the material is thermally stable.

All of the samples presented a similar behavior when submitted to the heat treatment. First of all, the evaporation of some water molecules in the silica surface is detected, and then occurs the degradation of the polymeric chains surround the rare earth ion. With the degradation of the organic material, it is supposed that the Eu^{3+} ion is possibly incorporated by the silica matrix.

The synthesis process was accompanied by the emission and excitation spectra of the Eu^{3+} ion in the encapsulated material. This technique allows us a better determination of the interactions around the Eu^{3+} ions than in the X ray technique, for example, which detects only the long-range interactions.

Figure 6 presents the excitation spectrum (A) and the emission spectrum (B) of the Eu_2O_3 . From the excitation

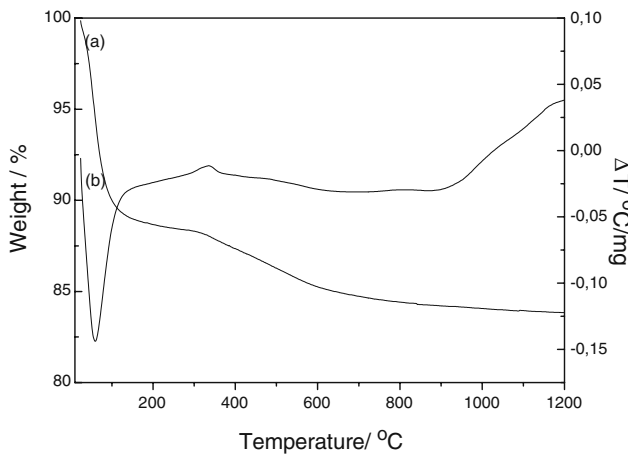


Fig. 5 (a) TGA e (b) DTA curves of the SiO₂@Eu₂O₃ spherical sample annealed at 100 °C

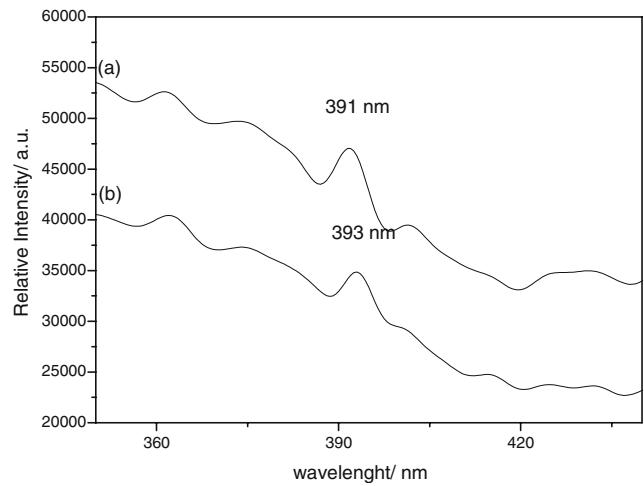


Fig. 7 Excitation spectra of the SiO₂@Eu₂O₃ FUMED (a) and the SiO₂@Eu₂O₃ spherical (b) samples annealed at 800 °C, λ_{em}=610 nm

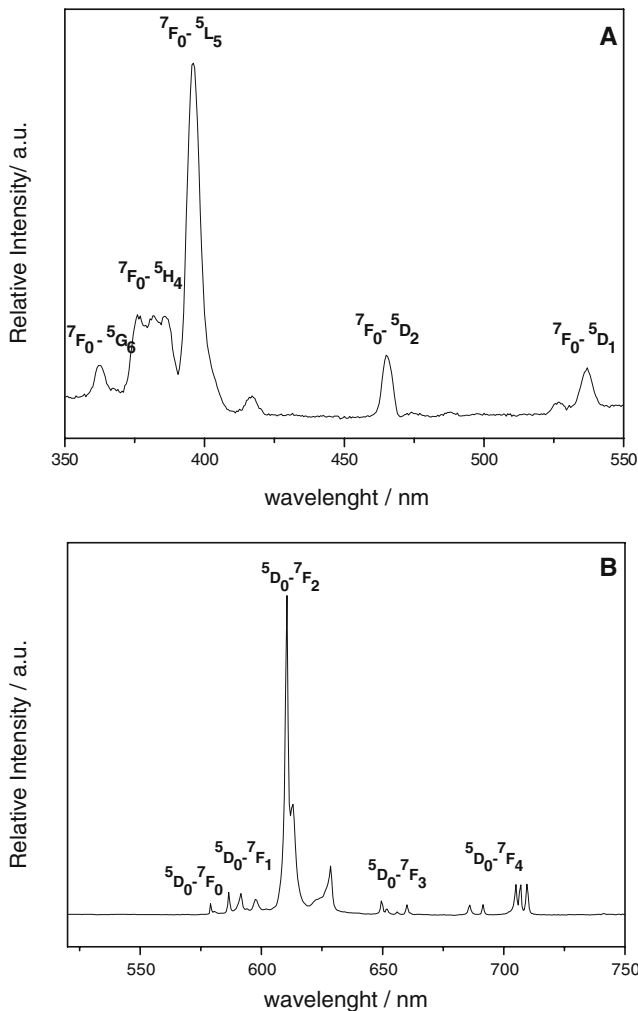


Fig. 6 Excitation spectrum (λ_{em}=610 nm) (a) and Emission spectrum (λ_{exc}=394 nm) (b) of the Eu₂O₃, at room temperature

spectrum (Fig. 6a) it is observed the narrow bands attributed to the 4f [6] intraconfigurational transitions, from the ground state ⁷F₀ to the excited states ⁵G₆ at 361 nm, ⁵H₄ at 381 nm, ⁵L₆ at 396 nm, ⁵D₂ at 465 nm and ⁵D₁ at 536 nm [20].

Normally, in inorganic systems, where the Eu³⁺ ion is excited by a light source of 394 nm (⁷F₀→⁵L₆) occurs a non radiative decay to the ⁵D levels, where the main level is the ⁵D₀, from which the ground state is reached, and bands of the ⁷F_J (J=0, 1, 2, 3, 4, 5, 6) levels are visualized at the emission spectrum [21]. Figure 6b presents the emission spectra of the Eu₂O₃ oxide, where is visualized the characteristic bands of the Eu³⁺ ion related to the decay of radiation from the state ⁵D₀→⁷F_J (J=0, 1, 2, 3, 4) in approximately 579, 591, 610, 650 e 707 nm, respectively, which the most intense band is related to the ⁵D₀→⁷F₂ transition at 610 nm.

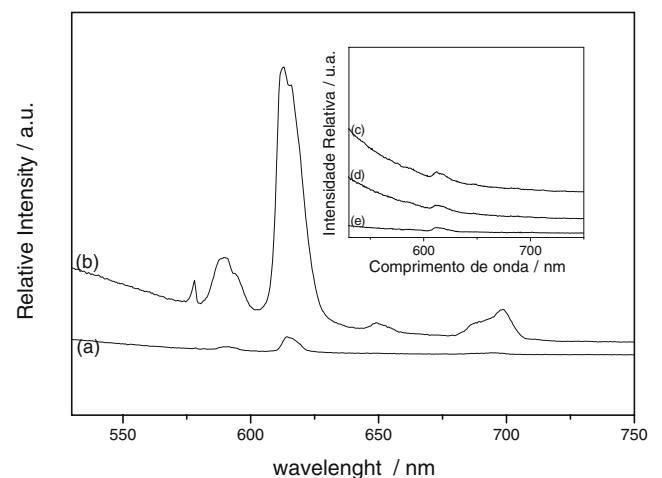


Fig. 8 Emission spectra of the SiO₂@Eu₂O₃ FUMED samples annealed at (a) 100, (b) 300 °C. Inset: (c) 400, (d) 500, (e) 800 °C, λ_{exc}=393 nm, at room temperature

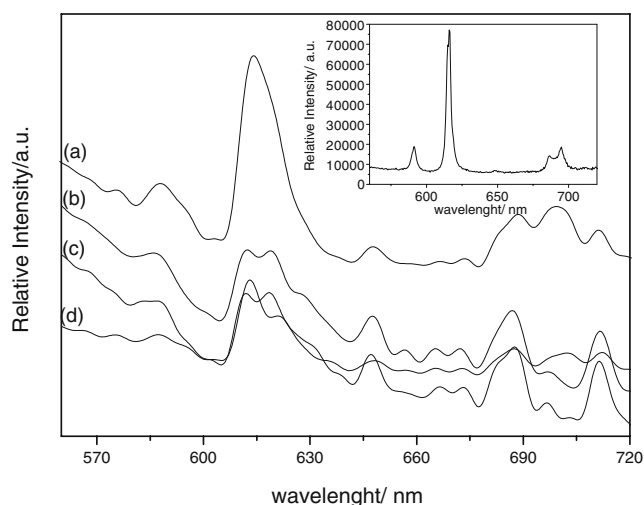


Fig. 9 Emission spectra of the $\text{SiO}_2@Eu_2O_3$ spherical samples annealed at 300 (a), 400 (b), 500 (c), and 800 °C (d). Insert: $\text{SiO}_2@Eu_2O_3$ spherical sample heat treated at 100 °C. $\lambda_{exc}=394$ nm, at room temperature

Figure 7 presents the excitation spectra of the $\text{SiO}_2@Eu_2O_3$ FUMED (Fig. 7a) and the $\text{SiO}_2@Eu_2O_3$ spherical sample (Fig. 7b) annealed at 800 °C. In both emission spectra appears a broad absorption band with a maximum at 393 nm. As it is shown in the excitation spectrum of the Eu_2O_3 (Fig. 6a), this band is related to the ${}^7F_0 \rightarrow {}^5L_6$ transition of the Eu^{3+} ion, which indicates that in the encapsulated material the mainly emission is proportionated by the rare earth ion.

Figure 8 presents the emission spectra of the $\text{SiO}_2@Eu_2O_3$ FUMED samples annealed at 100 (a), 300 (b). Insert: 400 (c), 500 (d) and 800 °C (e). At the Eu^{3+} emission spectrum obtained for the sample annealed at 300 °C ($\lambda_{exc}=393$ nm) the emission bands of this ion, related to the ${}^5D_0 \rightarrow {}^7F_J$ ($J=0, 1, 2, 3, 4$) transitions appeared at 577, 589, 612, 649 and 694 nm. The bands are resolved and intense, as it shows in the Eu_2O_3 emission spectrum (Fig. 6b), but they are not narrow, indicating the presence of different Eu^{3+} sites, probably due to the incorporation of the Eu^{3+} by the FUMED silica.

From the emission spectra presented at Fig. 8, it is seen an intensification in the bands relative intensity, when the sample was heated from 100 (a) to 300 °C (b), due to the degradation of the polymeric shell containing the Eu^{3+} .

The temperature enlargement causes losses of the organic groups and water molecules, which promotes a non radiative relaxation of the Eu^{3+} emission, which increases the intensity of emission. For the samples annealed upper than 300 °C, Fig. 8 (Insert (c), (d), (e)), however, they presented a subsequent Eu^{3+} ion emission quenching. In this case, it is supposed that this ion was also incorporated by the silica matrix, which posses some silanols groups that are responsible by this phenomena.

Figure 9 presents the emission spectra for the spherical silica, where it is observed the radiation decay from ${}^5D_0 \rightarrow {}^7F_J$ ($J=0, 1, 2, 3, 4$), and it appears at 577, 591, 616, 649 e 695 nm, respectively. The $\text{SiO}_2@Eu_2O_3$ spherical sample annealed at 100 °C (Fig. 9, Insert) presents the Eu^{3+} ion characteristic bands more intense than those noticed for the silica FUMED samples. From 100 to 300 and 400 °C happens a decrease in the relative intensity of these bands, due to the degradation of the polymeric organic shell involving the Eu^{3+} ion, as discussed above. In these spectra, the disappearance of the correspondent ${}^5D_0 \rightarrow {}^7F_0$ emission at 577 nm also indicates an environmental change around the rare earth ion as the temperature enhances. However, from 400 to 500 °C it was observed again an increase in the relative intensity of the ${}^5D_0 \rightarrow {}^7F_0$ emission at 577 nm, indicating another structural arrangement in the matrix, promoting the enhancement of the Eu^{3+} emissions, due to the interactions between this ion and the silica matrix.

The incorporation of the rare earth ions by the silica matrix during the encapsulation procedure it also studied by our group at ref 21. In this paper, a single layer of Eu_2O_3 was deposited over the $\text{SiO}_2\text{-GeO}_2$ VAD particles, and it was observed that the organic groups in the polymeric material containing the Eu^{3+} was degraded with the heat treatment, promoting some structural changes in the matrix, and around the 1000 °C, the Eu^{3+} was incorporated by the silica matrix via Ge-O-Eu, which causes the emission quenching of this ion. However in this presented work, the Eu^{3+} emission quenching with the temperature enhancement, was caused by the Si-OH groups in the silica surface.

In the FUMED silica surface, the Si-OH are homogenized dispersed and besides, they are located between the particles, promoting a stronger interaction with the Eu^{3+} than the observed for the Stöber silica, because its material

Table 1 Lifetime of the Eu^{3+} ${}^5D_0 \rightarrow {}^7F_2$ emission in the $\text{SiO}_2@Eu_2O_3$ FUMED and the $\text{SiO}_2@Eu_2O_3$ spherical samples

Temperature (°C)	Lifetime(ms) $\text{SiO}_2@Eu_2O_3$ FUMED	Lifetime(ms) $\text{SiO}_2@Eu_2O_3$ spherical
100	0.51	0.28
300	0.67	0.23
400	–	0.37
500	0.42	0.35
800	–	1.03

present the Si-OH groups only in the surface [22]. Besides the quenching caused by the silanols groups, it can be also caused by the agglomeration in the $\text{SiO}_2@\text{Eu}_2\text{O}_3$ spherical and the $\text{SiO}_2@\text{Eu}_2\text{O}_3$ FUMED [23].

The lifetime of the $^5\text{D}_0 \rightarrow ^7\text{F}_2$ emission of the Eu^{3+} ion for the $\text{SiO}_2@\text{Eu}_2\text{O}_3$ FUMED and the $\text{SiO}_2@\text{Eu}_2\text{O}_3$ spherical, were measured through the decay curves which presents a monoexponential feature (Table I). With the temperature increase there is a reduction in the lifetime of the Eu^{3+} emission, caused by the presence of hydroxyl groups and Si-OH on the surface of silica. These groups have different vibration levels, whose energies are located between the excited $^5\text{D}_0$ and the $^7\text{F}_6$ ground level. This means that there is a non-radiative loss of Eu^{3+} for these grupos [24].

The lifetime for a sample of pure Eu_2O_3 heated at 900 °C for 2 h was 0.16 ms. Comparing this result with the other samples, it is improved that the Eu^{3+} in the encapsulated material is first into an organic polymer matrix and, after heating treatment, in interaction with the silica matrix, and is not present in the form of pure oxide.

Conclusion

It was possible to conclude that the $^5\text{D}_0 \rightarrow ^7\text{F}_2$ hypersensitive transition is strongly dependent on the Eu^{3+} surrounding. With the temperature enhancement, occurs the polymeric shell degradation, that causes a structural changing around the Eu^{3+} ion, and because of this degradation, this ion is incorporated to the silica spherical and silica FUMED matrixes. It can be also observed through the lifetime values for the $\text{SiO}_2@\text{Eu}_2\text{O}_3$ spherical and $\text{SiO}_2@\text{Eu}_2\text{O}_3$ samples which presented a monoexponential feature.

Acknowledgements The authors gratefully acknowledge the agencies CAPES, FAPESP and CNPq. We also wish to thank Professor Osvaldo A. Serra from FFCLRP-USP for the photoluminescence measurements.

References

- Serra OA, Cicillini SA, Ishiki RR (2000) A new procedure to obtain Eu^{3+} doped oxide and oxosalt phosphor. *J Alloy Comp* 303–304:316–319
- Armellini C, Chiappini A, Chiasera A, Ferrari M, Jestin Y, Mortier M, Moser E, Retoux R, Righini GC (2007) Rare earth-activated silica based nanocomposites. *J Nanomaterials* 84745.
- Nassar EJ, Messaddeq Y, Ribeiro SJL (2002) Influência da catálise ácida e básica na preparação de sílica funcionalizada. *Quim Nova* 25(1):37–41
- Yu M, Lin J, Fang J (2005) Silica spheres coated with $\text{YVO}_4:\text{Eu}^{3+}$ layers via sol-gel process: A simple method to obtain spherical core-shell phosphors. *Chem Mater* 17:1783–1791
- Jia PY, Liu XM, Yu M, Luo Y, Fang J, Lin J (2006) Luminescent properties of sol-gel derived spherical $\text{SiO}_2@\text{Gd}_2(\text{WO}_4)_3:\text{Eu}^{3+}$ particles with core-shell structure. *Chem Phys Lett* 424:358–363

- Stöber W, Fink A, Bohn E (1968) Controlled growth of monodispersed silica spheres in the micron size range. *J Colloidal Interface Sci* 26:62–69
- Chen SL, Dong P, Yang GH, Yang JJ (1996) Kinetics of formation of monodisperse colloidal silica particles through the hydrolysis and condensation of tetraethylortosilicate. *Ind Eng Chem Res* 35:4487–4493
- Lee K, McCormick A (2005) Effect of pH on the final connectivity distribution of the silicon atoms in the Stöber particles. *J sol-gel Sci Tech* 33:255–260
- De Oliveira E, Neri CR, Serra OA, Prado AGS (2007) Antenna Effect in Highly Luminescent Eu^{3+} Anchored in Hexagonal Mesoporous Silica. *Chem Mater* 19:5437–5442
- Kalele S, Gosavi SW, Urban J, Kulkarni SK (2006) Nanoshell particles: synthesis, properties and applications. *C Science* 91:1038–1052
- Enrich F, Trave E, Bersani M (2008) Acid Synthesis Amine-functionalized or Erbium-doped silica spheres for biological applications. *J Fluoresc* 18(2):507–511
- Hall SR, Davis SA, Mann S (2000) Encapsulation of nanosized silica by in situ polymerization of tert-butyl acrylate monomer. *Langmuir* 16:1454
- Schuelz P, Caruso F (2002) Eletrostatically Assembled Fluorescent thin films of Rare-earth-doped Lanthanum phosphate Nanoparticles. *Chem Mater* 14:4509
- Sondi I, Fedynshyn TH, Sinta R, Mantijevic E (2000) Cocondensation of Organosilica Hybrid Shells on Nanoparticle Templates: A Direct Synthetic Route to Functionalized Core-Shell Colloids. *Langmuir* 16:9031
- Zhong Z, Mastai Y, Koltipin Y, Zhao Y, Gedanken A (1999) Sonochemical Coating of Nanosized Nickel on Alumina Sub-microspheres and the Interaction between the Nickel and the Nickel Oxide with the Substrate. *Chem Mater* 11:2350
- Li G, Wang Z, Quan Z, Li C, Lin J (2007) Growth of highly crystalline $\text{CaMoO}_4:\text{Tb}^{3+}$ phosphor layer on spherical SiO_2 particles via sol-gel process: Structural characterization and luminescent properties. *Cryst Growth Des* 7:1797–1802
- Liu XM, JIA PY, LI GZ, YU M, FANG J, LIN J (2006) Sol-gel synthesis and characterization of $\text{SiO}_2@\text{CaWO}_4$, $\text{SiO}_2@\text{CaWO}_4:\text{Eu}^{3+}/\text{Tb}^{3+}$ core-shell structured spherical particles. *Nanotechnology* 17:734–742
- Leite ER, Maciel AP, Weber IT, Lisboa-Filho PN, Longo E, Paiva-Santos CO, Andrade AVC, Maniette Y, Schreiner W (2002) Development of Metal Oxide Nanoparticles with High Stability Against Particle Growth Using a Metastable Solid Solution. *Adv Mater* 14:905–908
- Maciel AP, Leite ER, Longo E, Varela JA (2005) Método sol-gel modificado para obtenção de alumina nanoencapsulada com terras raras. *Cerâmica* 51:52–57
- Teotonio EES, Felinto MCFC, Brito HF, Malta OL, Trindade AC, Najjar R, Streck W (2004) Synthesis, crystalline structure and photoluminescence investigations of the new trivalent rare earth complexes (Sm^{3+} , Eu^{3+} and Tb^{3+}) containing 2-thiophenecarboxylate as sensitizer. *Inorg Chem Acta* 357:451–460
- Rosa ILV, Oliveira LH, Suzuki CK, Leite ER, Varela JA, Longo E (2008) $\text{SiO}_2\text{-GeO}_2$ soot preform as a core for Eu_2O_3 Nanocoating: Synthesis and Photophysical study. *J Fluorescence* 18:151–155
- Liu CC, Maciel GE (1996) The FUMED silica surface: A study by NMR. *J Am Chem Soc* 118:5103–5119
- Nogami M (2001) Fluorescence properties of Eu-doped $\text{GeO}_2\text{-SiO}_2$ glass heated under an H_2 atmosphere. *J Luminescence* 92:329–336
- Serra OA, Nassar EJ, Zapparolli G, Rosa ILV (1994) Organic complexes of Eu^{3+} supported in functionalized silica gel: highly luminescent material. *J Alloy Comp* 207–208:454–456